

Document downloaded from:

<http://hdl.handle.net/10251/57810>

This paper must be cited as:

Sánchez Diana, LD.; Sanchis Kilders, P. (2013). Broadband 8 micrometers long hybrid silicon-plasmonic transverse magnetic-transverse electric converter with losses below 2 dB. *Optics Letters*. 38(15):2842-2845. doi:10.1364/OL.38.002842.



The final publication is available at

<http://dx.doi.org/10.1364/OL.38.002842>

Copyright Optical Society of America

Additional Information

This paper was published in *Optics Letters* and is made available as an electronic reprint with the permission of OSA. The paper can be found at the following URL on the OSA website: <http://dx.doi.org/10.1364/OL.38.002842>. Systematic or multiple reproduction or distribution to multiple locations via electronic or other means is prohibited and is subject to penalties under law

Broadband 8 μm -long hybrid silicon-plasmonic TM-TE converter with losses below 2dB

L.Sánchez and P.Sanchis*

Nanophotonics Technology Center, Universitat Politècnica de València, Camino de Vera s/n,46022, Valencia, Spain

*Corresponding author: pabsanki@ntc.upv.es

A novel ultra-compact (8 μm length) hybrid silicon-plasmonic TM-TE converter is reported. The conversion is achieved during a partial power coupling between a waveguide and a hybrid plasmonic parallel waveguide. The impact of different types of metals is also analyzed. At a wavelength of 1.55 μm , the device has an extinction ratio of 27.6 dB and insertion losses of 1.75 dB. Furthermore, an optical bandwidth as large as 100 nm is achieved with extinction ratios higher than 25 dB and insertion losses below 2 dB. © 2013 Optical Society of America
OCIS Codes: 250.5300, 230.3120, 230.5440, 230.7370, 240.6680, 250.5403.

Silicon has dominated the electronics industry for the last decades and actually is taking a prominent role as key material for photonic integration. The main reason behind is the ability to adapt its fabrication to the well known CMOS fabrication process developed by the electronics industry [1]. This allows the integration of silicon photonics with electronics and makes possible the mass production of cost-effective devices. However, the high index contrast between silicon and its oxide causes polarization-dependent performance and the lower bound on the dimensions is limited by diffraction.

Surface-plasmon polaritons (SPPs) is a light propagation at the interface between a metal and a dielectric, based on hybrid electron-photon oscillation and it has been proposed for downscaling silicon photonic devices beyond the diffraction limit [2-3]. SPPs provide a large confinement of the light wave so they can reduce the footprint of photonic components and minimize the size mismatch with nanoscale electronics. But, on the other hand, they suffer from high propagation losses due to the field concentrated in the metal. Current works have proposed different ways to reduce propagation losses in plasmonic structures like enhanced waveguide guiding structures [4] or electric pumping in an active gain medium [5].

Other crucial topic in optical devices is the polarization management [6]. This issue is especially important to ensure the correct performance in receivers for optical communication systems because it is necessary to achieve the corresponding polarization for each type of device. Polarization circuits in silicon photonics have been largely studied and demonstrated. They are mainly based on devices like rotators [7,8] or converters [9]. H. Zhang *et al.* reported a rotator based on a horizontal slot waveguide showing an extinction ratio (ER) above 14 dB for a device length of 100 μm [7]. A rotator based on the symmetry breaking of the waveguide cross section was presented by M. Aamer *et al.* Their device was only 25 μm long and it has insertion losses (IL) ranging from 1dB to 2.5 dB over a wavelength range of 30 nm [8]. K. Nakayama *et al.* presented a TE-TM converter with an ER of 15 dB and a

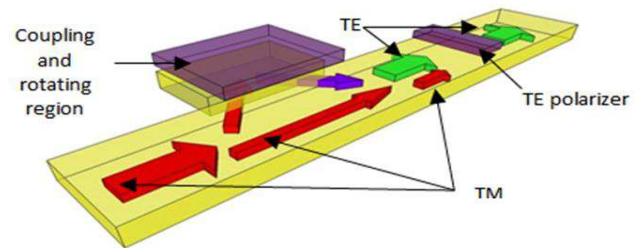


Fig. 1. Three-dimensional schematic of the TM-TE converter and its performance. The arrows represent the TM and TE components evolution. Red arrows are TM component and green arrows are TE component.

97% mode conversion but with a total length around 600 μm [9].

In recent times there have been developed new topologies based on plasmonic technology to drastically reduce the dimensions of the rotators [10,11]. M. Komatsu *et al.* showed theoretically the possibility of reaching, for a 11 μm -long plasmonic rotator, an ER of 20 dB and an IL of 4.7 dB for both polarization conversions [10]. On the other hand, J. Niklas *et al.* reported simulation results of an ultra-compact plasmonic rotator of 5 μm with an ER>14 dB and an IL of 2.1 dB [11]. In this work, we propose a novel ultra-compact and low-loss TM-TE converter topology based on hybrid silicon-plasmonic technology. Table 1 shows the comparison with respect to the state of the art. The proposed device has a total length of 8 μm and improves the ER up to 27.6 dB, while maintaining the IL as low as 1.75 dB, at the standard telecom wavelength of 1550 nm. Furthermore, the device exhibits a broadband optical bandwidth of 100 nm where the ER remains above 25 dB and the IL below 2 dB.

Table 1. Comparison with the state of the art.

$\lambda=1.55 \mu\text{m}$	Ref [10]	Ref [11]	Our work
Extinction ratio (dB)	20	14	27.6
Insertion losses (dB)	4.7	2.1	1.75
Device length (μm)	11	5	8

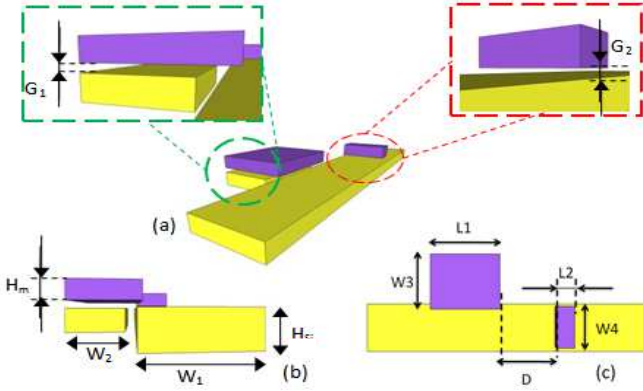


Fig. 2. (a) Three-dimensional schematic of the whole structure. (b) Front view. (c) Top view.

The device is shown in Fig. 1. It has two metallizations; the first one is used to rotate the TM mode into a TE mode while the second one is used to minimize the residual TM component at the output. Such simple rectangular metallizations can be fabricated by standard processing steps and contribute to increase the robustness of the device against potential fabrication inaccuracies by avoiding the use of sharp angles in the metallization [10] or the metal rotation around the silicon waveguide [11]. Fig. 2 shows the dimensions of the structure. The metallizations have a cross section of $W_3 \times H_m$ and $W_4 \times H_m$ respectively. The input waveguide is 500×220 nm ($W_1 \times H_{si}$) and the parallel waveguide has a cross section of 400×220 nm ($W_2 \times H_{si}$). The separation between the central waveguide and the hybrid plasmonic parallel waveguide is 50 nm. The height of the metallizations is 200 nm (H_m) and the height of the SiO_2 gaps is 50 nm and 20 nm (G_1 and G_2 respectively). Other final dimensions are $L_1=5$ μm , $L_2=1$ μm , $W_3=500$ nm and $W_4=350$ nm. The first metallization, corresponding to the coupling region, has a constant overlapping of 50 nm over the input waveguide. The distance between the metallizations (D) is 2 μm . Fig. 3 shows the principal steps of the design process. Three-dimensional (3D) finite-difference time-

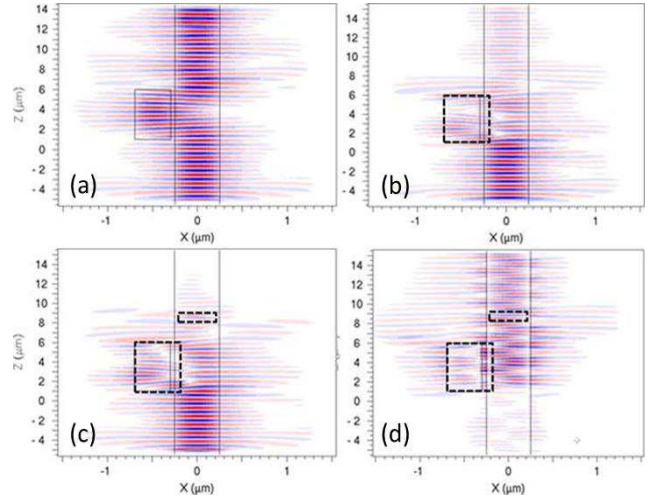


Fig. 4. For TM input polarization, TM contour map for (a) structure without metallizations, (b) with the first metallization for achieving TM-TE conversion and (c) with the second metallization for minimizing the residual TM component at the output. (d) TE contour map with the two metallizations showing the TM-TE conversion. The metals are copper in all cases.

domain (FDTD) simulations have been carried out for the design. Two different metals have been analyzed: silver ($n=0.514+10.8j$ [12]) and copper ($n=0.282+11.048j$ [13]). The first step is the design of the polarization converter without the polarizer. The coupling between two parallel waveguides is exploited to achieve the rotation from TM to TE polarization without changing the metallization shape. To achieve this goal, the parallel waveguide is initially designed without the metal to achieve that, for a length L_1 of 5 μm , the input TM mode is coupled into the parallel waveguide and back to the input waveguide for such a length, as depicted in Fig. 4(a). The introduction of the metal on top of the parallel waveguide is then used to achieve the TM-TE polarization conversion. The physics behind is similar to previous works [10,11]. The electric field at the hybrid structure tends to stay normal to the metallic surface. Therefore, when light is gradually

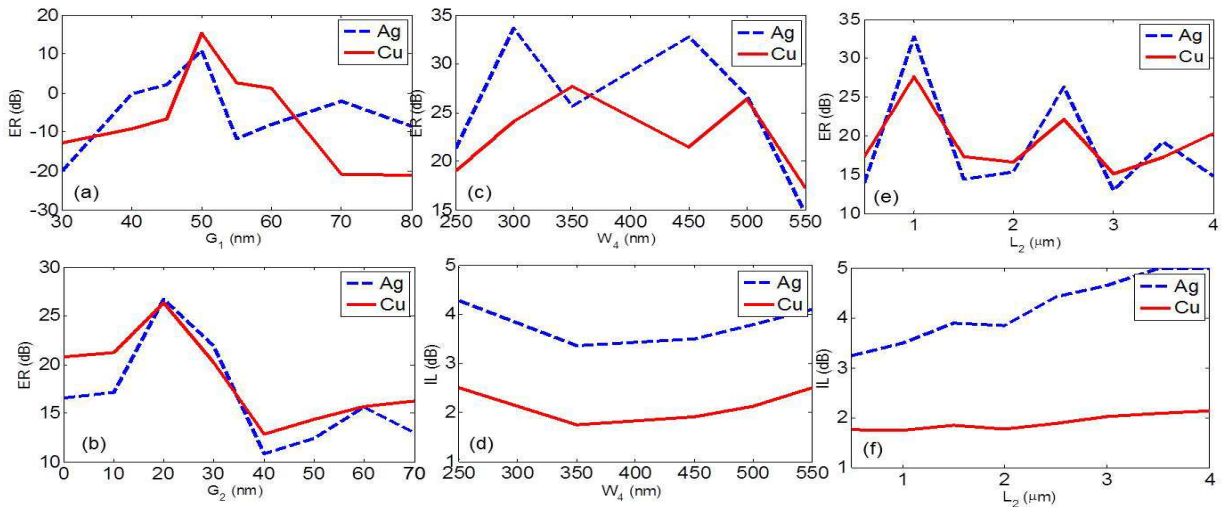


Fig. 3. Principal steps of the design process.

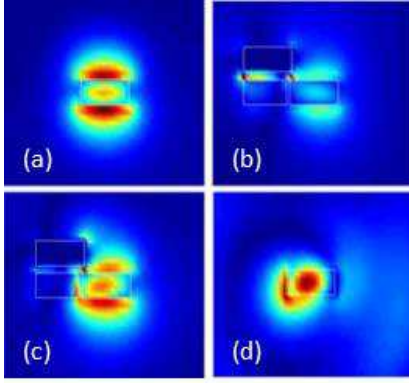


Fig. 5. Norm of the electric field ($|\vec{E}|$) is shown at the input (a), output (d) and two intermediate positions of the hybrid plasmonic parallel waveguide (b and c).

coupled back from the hybrid plasmonic parallel waveguide to the silicon waveguide, the electric field tries to continue being normal to the metallic surface. In such a way, the vertical component of the electric field is gradually rotated into a horizontal component thus converting the input TM polarization into a TE polarization. This effect is clearly seen in Fig. 5 where the norm of the electric field ($|\vec{E}|$) is shown at the input, output and two intermediate positions of the hybrid plasmonic parallel waveguide. The input TM mode, Fig. 5(a), becomes confined below the metal when is coupled to the hybrid plasmonic parallel waveguide, Fig. 5(b). As the mode starts to couple again back to the silicon waveguide, Fig. 5(c), the electric field tries to continue being normal to the metallic surface and thus the mode is gradually rotated. Therefore, the polarization of the mode at the output waveguide, Fig. 5(d), is converted to TE. The optimum values of W_3 and G_1 parameters have been analyzed by means of simulations. The highest ER is achieved for $W_3=500$ nm, in which the metallization is partly overlapping the input waveguide, while it decreases below and above this value. Furthermore, the minimum IL is also achieved for this width. The optimum G_1 has then been analyzed. Fig. 3(a) shows the variation of ER as a function of the gap for the different metals. A positive ER means that at the output of the coupling region we have more TE component than TM component and therefore the conversion is happening. The best ER is obtained for $G_1=50$ nm for both metals. In this case, an ER of 10.97 dB and IL of 3.18 dB are achieved for silver while an ER of 15.32 dB and IL of 1.54 dB are achieved for copper. Fig. 4(b) shows the TM contour map of the optimized hybrid plasmonic parallel waveguide with copper. It can be seen that there is still a residual TM component at the output.

The next step is thus improving the ER with the TE pass polarizer, which consists of a metal layer on top of the silicon waveguide. In such hybrid plasmonic waveguide, the TM mode is mostly confined between the silicon waveguide and the metallization and therefore is highly attenuated when propagating. On the other hand, the TE mode is mostly confined in the silicon waveguide and therefore less affected by the metallization. In our case, as the TM component at the

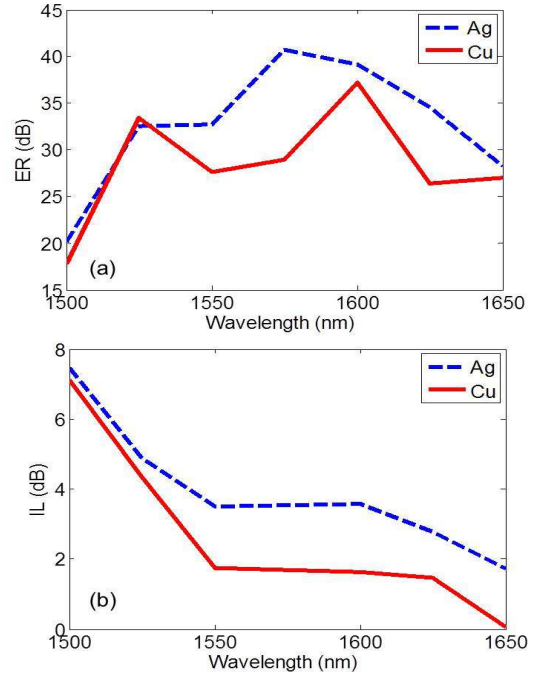


Fig. 6. (a) Extinction ratio versus wavelength. (b) Insertion loss versus wavelength.

output of the TM-TE converter is also significantly attenuated, as it was shown in Fig. 4(b), a very short length of only $1 \mu\text{m}$ is required as compared to the $30 \mu\text{m}$ length reported for the isolated polarizer [14]. Initially, we consider the same width for the polarizer metallization than for the silicon waveguide ($W_4=500$ nm) and analyze the influence of the polarizer gap. As shown in Fig. 3(b), the best ER obtained is for a gap G_2 of 20 nm for both metals. With silver, we obtain an ER of 26.7 dB and in the case of copper, the ER reaches 26.3 dB. The next step of the design process is to optimize the dimensions of the polarizer to improve the ER and the IL. As shown in Fig. 3(c) and Fig. 3(d), for silver we achieve the best trade-off between ER and IL for a width W_4 of 450 nm (ER=32.76 dB and IL=3.5 dB) while in the case of copper the best trade-off is for 350nm with an ER=27.6 dB and IL=1.75 dB. In any case, with the polarizer width optimized for each metal, we have also analyzed the influence of the polarizer length in the performance of the device. We can see in Fig. 3(e) and Fig. 3(f) that the best trade-off for both metals is for $L_2=1 \mu\text{m}$. The performance of the optimized device is shown in Fig. 4(c) and (d) for copper. It can be seen that the TM polarization is suppressed after the polarizer while the TE component appears after the TM-TE converter and crosses the polarizer without noticeable losses.

Fig. 6 shows the wavelength response of the optimized device with copper and silver. In view of these results, we choose copper instead silver for the metallizations. Though the device with silver has a better ER for a wavelength of 1550nm, it also has more IL (ER=32.76dB and IL=3.5dB). The reason is that although silver has a smaller value of the imaginary part of the refractive index, insertion losses are higher than in copper due to

the larger value of the real part of the refractive index. The higher index makes that the TE component is more influenced by the metal in the polarizer thus increasing its propagation losses. Therefore, by considering copper in the metallizations we have a rather high ER and the IL are below 2dB (ER=27.6dB and IL=1.75dB). Hence, the proposed TM-TE converter has an ER greater than 25dB and IL below 2dB for a bandwidth between 1550nm and 1650nm.

In summary, an ultra-compact, low-loss and broadband TM-TE converter has been designed for enabling polarization diversity in silicon photonic circuits. The impact of different metals have been analyzed and copper has been chosen as the best option to minimize insertion losses which in turn will also ensure CMOS processing compatibility.

Acknowledgements

Authors acknowledge funding from TEC2012-38540 LEOMIS and PROMETEO-2010-087. L.Sánchez also acknowledges the Generalitat Valenciana for funding his grant in the context of the VALi+d program.

References

- 1.B.Jalali and S.Fathpour, *IEEE Journal of lightwave Tecnology*, **24**, 4600 (2006)
- 2.J.A.Dionne, L.A.Sweatlock, M.T.Sheldon, A.P.Alivisatos and H.A.Alwater, *IEEE Journal of Selected Topics in Quantum Electronics*, **16**, 295 (2010).
- 3.S.Zhu, G.Q.Lo and D.L.Kwong, *IEEE Photonics Technology Letters*, **24**, 1224 (2012).
- 4.L.Y.M.Tobing, L.Tjahjana and D.H.Zhang, *Applied Physics Letters*, **101**, 1117 (2012).
- 5.D.Y.Fedyanin, A.V.Krasavin, A.V.Arsenin and A.V. Zayats, *Nano Letters*, **12**, 2459(2012).
- 6.C.A.Ramos, R.Halir, A.O.Moñux, P.Cheben, L.Vivien, I.M.Fernández, D.M.Morini, S.Janz, D.X.Xu and J.Schmid, *Optics Letters*, **37**, 3534 (2012).
- 7.H.Zhang, S.Das, Y.Huang,C.Li and S.Chen, *Applied Physics Letters*, **101**,021105-1 (2012).
8. M. Aamer, A. M. Gutierrez, A. Brimont, D.Vermeulen, G. Roelkens, J.M.Fedeli, A. Håkansson and P. Sanchis, *IEEE Photonics Technology Letters*, **24**, 2031 (2012).
- 9.K.Nakayama, Y.Shoji and T.Mizumoto, *IEEE Photonics Technology Letters*, **24**, 1310 (2012).
10. M.Komatsu, K.Saitoh and M.Koshiba, *IEEE Photonics Journal*, **4**, 707, (2012).
- 11.J.N.Caspers, M.Z.Alam and M.Mojahedi, *Optics Letters*, **37**, 4615(2012).
- 12.E.D.Palik, in "Handbook of Optical Constants of Solids", (E.D.Palik ed.), Academic Press, Orlando, Florida (1985)
13. S.Roberts, *Physical Review*, **118**,1509 (1960)
- 14.X.Sun, M.Z.Alam, S.J.Wagner, J.S. Aitchison and M.Mojahedi, *Optics Letters*, **37**, 4814 (2012).